Eur. J. Mineral.
2010, **22**, 613–621
Published online May 2010

Arsenoflorencite-(La), a new mineral from the Komi Republic, Russian Federation: description and crystal structure

STUART J. MILLS[1,*], PAVEL M. KARTASHOV[2], ANTHONY R. KAMPF[3] and MATI RAUDSEPP[1]

[1] Department of Earth and Ocean Sciences, University of British Columbia, Vancouver, BC V6T 1Z4, Canada
*Corresponding author, e-mail: smills@eos.ubc.ca
[2] Institute of Geology Ore Deposits, Petrography, Mineralogy and Geochemistry of the Russian Academy of Sciences, Staromonetnyi pereulok 35, 119017 Moscow, Russia
[3] Mineral Sciences Department, Natural History Museum of Los Angeles County, 900 Exposition Boulevard, Los Angeles, CA 90007, USA

Abstract: Arsenoflorencite-(La) [Арсенфлоренсит-(La)], ideally $LaAl_3(AsO_4)_2(OH)_6$, is a new mineral (IMA2009–078), from the Grubependity Lake cirque, Maldynyrd range, upper Kozhim River basin, Prepolar Ural, Komi Republic, Russia. It occurs in direct association with zircon, quartz, hematite, ardennite-(As), andalusite, anorthite, sericite, clinochlore, chernovite-(Y), manganiandrosite-(La), spessartine and monazite–gasparite-group minerals in Mn-rich nodules in metasediments. Arsenoflorencite-(La) forms orange–red to pink rhombohedral, pseudocubic or tabular crystals up to about 0.2 mm across. The dominant forms observed are {001} and {102}. The crystals have a vitreous lustre, are transparent to translucent, have a very light pink streak and are non-fluorescent. Mohs hardness is about 3.5 (estimated). The fracture is uneven and the tenacity is brittle. Arsenoflorencite-(La) has fair cleavage on {001}. Crystals are uniaxial (+), with the indices of refraction $\omega = 1.740(5)$ and $\varepsilon = 1.750(5)$, measured in white light, and are nonpleochroic. The empirical formula (based on 14 O atoms) is: $(La_{0.56}Ce_{0.18}Nd_{0.12}Pr_{0.04}Sr_{0.09}Ca_{0.03})_{\Sigma 1.02}(Al_{2.94}Fe_{0.06})_{\Sigma 3.00}(As_{1.80}P_{0.21})_{\Sigma 2.01}H_{5.95}O_{14}$. The simplified formula is $LaAl_3(AsO_4)_2(OH)_6$. Arsenoflorencite-(La) is trigonal, space group $R\bar{3}m$, $a = 7.0316(3)$, $c = 16.5151(8)$ Å, $V = 707.16(5)$ Å^3 and $Z = 3$. The crystal structure was solved from single-crystal X-ray diffraction data and refined to $R_1 = 0.0112$ on the basis of 287 unique reflections with $F_o > 4\sigma F$ and $R_1 = 0.0116$ for all 293 reflections. The five strongest lines in the powder X-ray diffraction pattern are [d_{obs} in Å, (I), (hkl)]: 2.982, (100), (113); 3.538, (55), (110); 1.914, (38), (303, 033); 2.211, (28), (122); 5.755, (27), (101). The name is for its relationship to florencite [and arsenoflorencite-(Ce)] with La as the dominant REE.

Key-words: arsenoflorencite-(La), Grubependity Lake cirque, Prepolar Ural, Komi Republic, crystal structure, alunite supergroup, lanthanum aluminium arsenate hydroxide, new mineral.

1. Introduction

Members of the alunite supergroup are studied widely, and have importance not only to mineralogy (*e.g.*, in acid mine drainage – Nordstrom *et al.*, 2000; mobility of toxic elements – Kolitsch & Pring, 2001), but also to metallurgical processing (*e.g.*, Dutrizac & Jambor, 2000), and have also been recently identified on the surface of Mars (*e.g.*, Klingelhöfer *et al.*, 2004). More recently, the nomenclature of the alunite supergroup has been revisited (Bayliss *et al.*, submitted) by the Commission on New Minerals, Nomenclature and Classification (IMA–CNMNC), and the alunite supergroup was also included as part of the new group-hierarchy classification (Mills *et al.*, 2009a).

Members of the alunite supergroup have the general formula $AB_3(XO_4)_2(OH,H_2O)_6$, where A is a large cation site containing cations such as Na^+, K^+, H_3O^+, Ba^{2+}, Sr^{2+}, Ca^{2+}, Pb^{2+} and REE^{3+}; B is an octahedral site containing typically Al^{3+} or Fe^{3+}, but it can also include V^{3+}, Ga^{3+}, Zn^{2+} and Cu^{2+}; and X is a tetrahedral site occupied by S, P or As (Scott, 1987; Jambor, 1999). Most alunite-related minerals have the rhombohedral space group $R\bar{3}m$, with hexagonal cell parameters $a_h \approx 7$ Å, $c_h \approx 17$ Å (*e.g.*, crandallite, Blount, 1974). The composition often requires modification to accommodate different combinations of cations. Such modifications include OH substitution for O in the XO_4 tetrahedron, substitution of H_2O or O for OH, and partial occupancy of the A and/or B sites (Jambor, 1999). Several unique modifications on the alunite structure-type have recently been described, which include the presence of trigonal bipyramidally coordinated Zn located within the six-membered rings in the octahedral layers in kintoreite (Grey *et al.*, 2009) and in the segnitite-related mineral

0935-1221/10/0022-2043 $ 4.05
DOI: 10.1127/0935-1221/2010/0022-2043

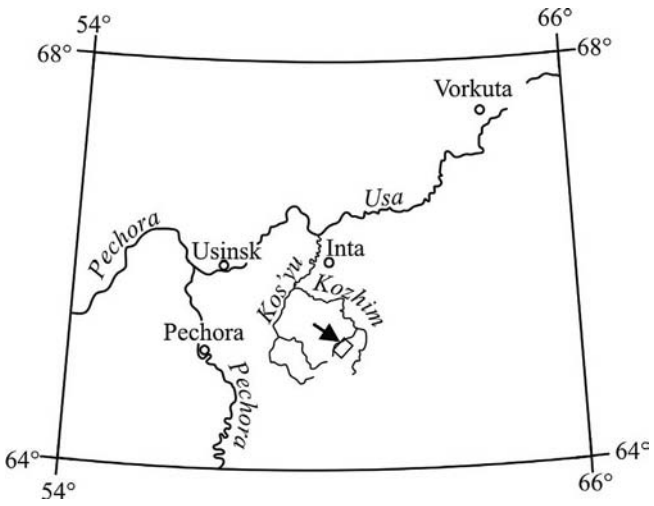

Fig. 1. Location of Grubependity Lake cirque, within the upper Kozhim River basin.

kolitschite (Grey *et al.*, 2008; Mills *et al.*, 2008; Mills & Birch, 2010), as well as the presence of crandallite-type blocks within the structure of perhamite (Mills *et al.*, 2006).

The type specimen and associated material was collected in the summer of 1999 by S.V. Surenkov at the Grubependity Lake cirque, Grubependity Lake, Maldynyrd range, upper Kozhim River basin, Prepolar Ural, Komi Republic, Russia (Fig. 1), several kilometres from the Chudnoe Pd–Au–Cr deposit. The mineral is named for its relationship to florencite [and arsenoflorencite-(Ce)] with La as the dominant REE, in accord with rare-earth nomenclature (Levinson, 1966). Arsenoflorencite-(La) is a member of the dussertite group in the alunite supergroup (Mills *et al.*, 2009a). The mineral and name have been approved by the IMA–CNMNC (IMA 2008–078). One co-type specimen is housed in the collections of Mineral Sciences Department, Natural History Museum of Los Angeles County (900 Exposition Boulevard, Los Angeles, California 90007, USA), catalogue number 62567, and one in the collections of the Fersman Mineralogical Museum (Leninskiy Prospekt 18(2), Moscow 117071, Russia), registered number 3891/1.

2. Occurrence and paragenesis

In the Maldynyrd range of the Prepolar Urals there are two large tectonic complexes; the Baikalian (Pre-Uralides) and Caledono–Hercynian (Uralides). The lower Uralides are represented by the Ordovician terrigenous Tel'poss (Obeiz) formation (O_1tp), whilst the upper Uralides are represented by Ordovician continental sediments of the Alkesvozh formation (ε-O_1al), including redeposited crust of the Vendian Period, which underlies both formations. These sequences are partially composed by diabases and dolerites of the Manaraga complex (βR_3-V) crosscut by rhyolites of Maldy complex ($\lambda\pi$V), however, the majority of the sequence comprises of metamorphosed effusive rocks of the Sablegorskaya formation (R_3-Vsb) (Fig. 2). These rocks were initially metamorphosed during the Early–Middle Cambrian, and underwent further metamorphism in the Late Paleozoic, under chlorite–muscovite conditions of the greenschist facies (~400 °C), with kyanite occurring along Paleozoic fault zones (Yudovich *et al.*, 2001). Arsenoflorencite-(La) and associated minerals are likely to have formed during recrystallisation of concretions in metasediment (see below) at this time.

The geology of the Grubependity Lake cirque area is complex. Both the Tel'poss and Alkesvozh formations are well exposed. The Alkesvozh sediments also share a contact with altered rhyolites and diabases of Vendian age, which are observed on slopes of the cirque. Mica–chloritoid schists, aporhyolite–pyrophyllite schists, conglomerates related to the Alkesvozh formation and diabases of the Manaraga complex (crosscut by the Malda rhyolite) are all exposed in the cirque; however, their relative geological positions have been displaced by tectonic events. This area was extensively explored in 1995–1996 because of the presence of gold (with contents of gold more than 1 kg/t).

In 1996, unusual concretions with REE mineralisation were found by L.I. Efanova in a layer of schist resulting from the metamorphism of coarse-granular arkosic sandstones (Yudovich *et al.*, 2000). The schist consists of quartz, chlorite, sericite and hematite with accessory ardennite-(As), spessartine and monazite-(Ce). Other minerals found

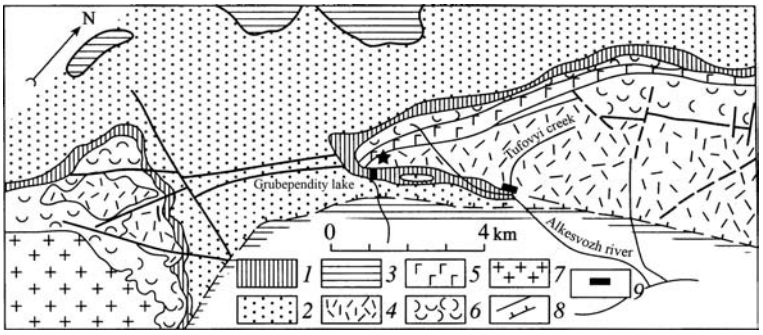

Fig. 2. Geological map of southern part of Maldynyrd range (after Yudovich *et al.*, 2000). 1 – Conglomerates and porphyroblastic chloritoid schists of the Alkesvozh formation (ε-O_1al), 2 – Conglomerates and quartzite-sandstones of Tel'poss (Obeiz) formation (O_1tp), 3 – Schists of Hydei (Saled) formation (O_1hd), 4 – Rhyolites of Maldy complex ($\lambda\pi$V), 5 – Dolerites of Manaraga complex (βR_3-V), 6 – Metabasites, rhyolites and tuffs of Sablegorskaya formation (R_3-Vsb), 7 – Granites of Maldinskii massif (γV), 8 – Faults and overthrusts, 9 – Sampling place.

in the schists include: epidote, allanite-(Ce), pyrophyllite, diaspore, piemontite, monazite-(La), florencite-(Ce), xenotime-(Y), chloritoid and gold. Macroscopically, the concretions are red-brown and vary from 3 × 5 to 30 × 10 cm across. They consist of the same minerals as the schist, but with higher concentration of Mn-bearing minerals – ardennite-(As), spessartine and piemontite. In addition, manganiandrosite-(La), zircon, monazite-(La), xenotime-(Y), chernovite-(Y), Nd-rich chernovite-(Y), gasparite-(Ce) and arsenoflorencite-(La) were detected in heavy mineral concentrates from the concretions. Three new Nd- and La-dominant LREE arsenates belonging to the chernovite and gasparite groups and an unnamed, probably new, high-Mn, Nd-dominant allanite-group mineral have also been identified.

Our investigation centers on a small 3 × 2 cm concretion, collected by S.V. Surenkov in 1999 from the same trench sampled by L.I. Efanova. Unfortunately, the concretion was crushed and we obtained samples as a set of fractions divided by heavy liquids and electromagnets. We are, therefore, unable to give a detailed petrographic description of the concretion. Its mineralogical associations were reconstructed on the basis of observed mineral intergrowths. The main difference between our sample and those described by Yudovich *et al.* (2000) is the complete absence of spessartine and any epidote-group minerals in our concretion. In this sample, arsenoflorencite-(La) occurs in direct association with zircon, quartz, hematite, ardennite-(As), andalusite, sillimanite, anorthite, sericite, clinochlore, chernovite-(Y), and monazite–gasparite-group minerals.

Arsenoflorencite-(La) also occurs at the Holičky, Stráž and Osečná deposits, North Bohemian Uranium District, Liberec Region, Bohemia, Czech Republic. Here it occurs in the cement of Cenomanian (99.6–93.5 Ma) sandstones as zones within crystals of florencite-(Ce) (irregular crystals which grade into arsenogoyazite) and zoned crystals with ''arsenoflorencite-(Nd)'' and crandallite (Scharm *et al.*, 1991).

3. Physical and optical properties

Arsenoflorencite-(La) forms orange–red to pink rhombohedral, pseudocubic or tabular crystals up to about 0.2 mm across (Fig. 3 and 4), which are visually indistinguishable from andalusite. Forms observed are {001} and {102}. Arsenoflorencite-(La) crystals are transparent to translucent, the streak is very pale pink. Crystals have a vitreous lustre and have fair cleavage on {001}. Mohs hardness is estimated at about 3.5, by analogy to other alunite supergroup minerals. The tenacity is brittle, the fracture is uneven and no parting was observed. No macroscopic or microscopic twinning was observed. The density measured by the sink-float method in Clerici solution is 4.15(5) g/cm^{-3}, whilst the calculated density from the empirical formula and single-crystal unit-cell is 4.159 g/cm^3. Arsenoflorencite-(La) is non-fluorescent under unfiltered ultraviolet light; however, some crystals change from pink to deep marine-green when elevated Nd contents are present. A similar green colour has been noted by one of the authors (PMK) for lanthanite-(Nd) from Japan and Pavlovskoe, Russia, and monazite-(Nd) from Switzerland and Sukhoi Log, Russia.

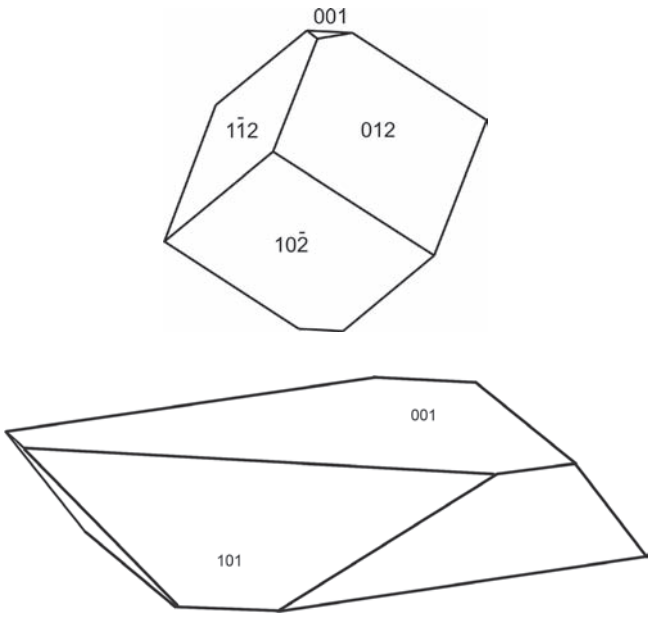

Fig. 3. Crystal drawing (clinographic projection) of the arsenoflorencite-(La) crystal used for structure determination and optical measurements (top) and crystal drawing of a typical arsenoflorencite-(La) crystal showing {001} and {101} (bottom).

Crystals of arsenoflorencite-(La) are uniaxial (+), with the indices of refraction $\omega = 1.740(5)$ and $\varepsilon = 1.750(5)$, measured in white light. Arsenoflorencite-(La) is nonpleochroic. Optical measurements were conducted on the crystal used for structure determination.

4. Chemical composition

Quantitative wavelength-dispersive electron-microprobe analyses (10 points on 9 separate grains) were carried out using a JSM-5610LV with an INCA-450 EDS attachment at IGEM, Russia. Operating conditions were 25 kV and 20 nA with a 5 μm beam diameter. No other elements were detected. H_2O could not be measured due to lack of material. The results, as well as the standards used, are shown in Table 1.

The empirical formula (based on 14 O atoms) is: $(La_{0.56}Ce_{0.18}Nd_{0.12}Pr_{0.04}Sr_{0.09}Ca_{0.03})_{\Sigma 1.02}(Al_{2.94}Fe_{0.06})_{\Sigma 3.00}(As_{1.80}P_{0.21})_{\Sigma 2.01}H_{5.95}O_{14}$. The simplified end-member formula is $LaAl_3(AsO_4)_2(OH)_6$, which requires La_2O_3 27.16, Al_2O_3 25.50, As_2O_5 38.32 and H_2O 9.01, total 100.00 wt%.

5. Powder X-ray diffraction

X-ray powder-diffraction data (Table 2) were collected on a Rigaku R-AXIS Spider curved-imaging-plate microdiffractometer utilising monochromatized Mo$K\alpha$ radiation at

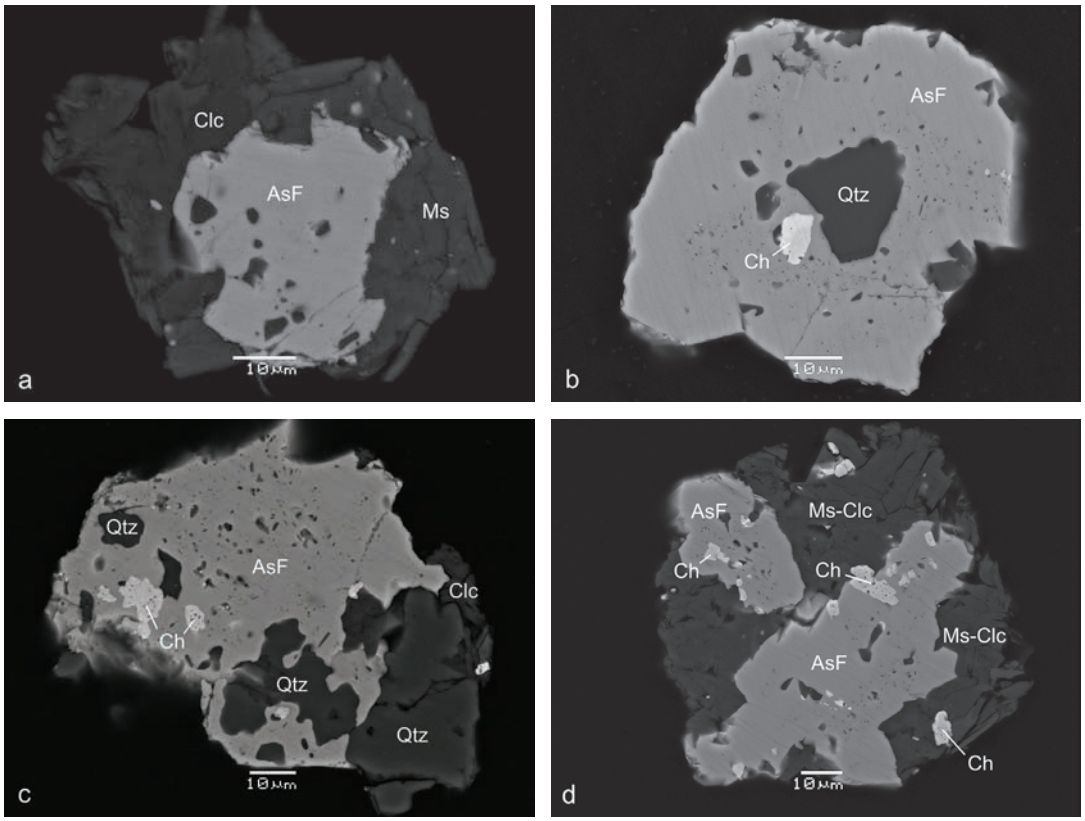

Fig. 4. Grains of arsenoflorencite-(La) with inclusions of chernovite-(Y), from the heavy fraction of the studied concretion. Mineral abbreviations: AsF = arsenoflorencite-(La), Clc = clinochlore, Ms = muscovite, Qtz = quartz and Ch = chernovite-(Y). (a) Arsenoflorencite-(La) (Table 7, analysis 1) grain within muscovite (grey) and clinochlore (dark-grey) plates without chernovite-(Y) inclusions; (b) arsenoflorencite-(La) (Table 7, anal. 2) grain with inclusions of chernovite-(Y) (bright, Table 7, anal. 3) and quartz (dark); (c) arsenoflorencite-(La) (Table 7, anal. 4) grain with inclusions of chernovite-(Y) (bright, Table 7, anal. 5) and quartz (dark) within a clinochlore matrix; (d) arsenoflorencite-(La) grain with inclusions of chernovite-(Y) of early generation (medium bright) and quartz (dark) within muscovite-clinochlore matrix containing chernovite-(Y) inclusions (very bright) of a later generation enriched in HREE.

Table 1. Analytical data for arsenoflorencite-(La).

Constituent	wt%	Min	Max	Standard dev.	Probe standard
CaO	0.29	0.00	1.64	0.55	Nacaphite
SrO	1.65	0.00	3.38	1.39	Synthetic $SrSO_4$
Al_2O_3	25.38	22.49	26.60	1.15	Synthetic Al_2O_3
Fe_2O_3	0.77	0.00	3.76	1.15	Chalcopyrite
La_2O_3	15.42	12.28	18.71	2.43	Synthetic $LaPO_4$
Ce_2O_3	5.01	3.10	7.49	1.61	Synthetic $CePO_4$
Pr_2O_3	1.17	0.00	2.22	0.83	Synthetic $PrPO_4$
Nd_2O_3	3.50	1.42	5.96	1.74	Synthetic $NdPO_4$
Sm_2O_3	0.00	0.00	0.00	0.00	Synthetic $SmPO_4$
MoO_3	0.12	0.00	1.21	0.38	Mo metal
P_2O_5	2.54	1.56	7.16	1.65	Nacaphite
As_2O_5	35.06	28.38	36.43	2.39	Sperrylite
Sum	90.90	90.60	91.07	0.13	
H_2O*	9.09	8.92	9.40	0.13	
Total	100.00	99.92	100.02	0.03	
REE_2O_3	25.10	21.95	28.46	2.12	

*Calculated for charge balance.

Table 2. X-ray powder diffraction data for arsenoflorencite-(La). I_{calc} is from crystal structure analysis and d_{calc} is from cell refined from powder data*.

I_{obs}	d_{obs}	d_{calc}	I_{calc}	*hkl*
27	**5.755**	5.741	25	101
15	5.567	5.533	15	003
55	**3.538**	3.532	54	110
7	3.446	3.434	4	104
100	**2.982**	2.977	100	113
3	2.871	2.870	2	202
10	2.767	2.767	13	006
5	2.462	2.462	5	024
2	2.291	2.290	2	205
28	**2.211**	2.211	24	122
19	**2.179**	2.178	17	116
8	2.037	2.039	7	300
6	2.019	2.020	8	214
38	**1.914**	1.914	35	303, 033
24	**1.767**	1.766	26	220
9	1.683	1.682	7	223
8	1.655	1.656	6	217
15	1.636	1.635	11	119
2	1.602	1.602	2	1.0.10
2	1.545	1.544	1	128
3	1.505	1.504	1	315
12	1.488	1.489	12	226
9	1.458	1.459	12	0.2.10
2	1.436	1.435	2	404
6	1.379	1.380	5	137
7	1.368	1.368	8	309, 039
3	1.348	1.348	3	2.1.10
18	**1.298**	1.298	16	413, 143

*Intensities ≥ 2 were calculated using PowderCell (Kraus & Nolze, 1996).
8 strongest lines are in bold-face.

Table 3. Summary of data collection conditions and refinement parameters for arsenoflorencite-(La).

Crystal data	
Cell parameters	$a = 7.0316(3)$ Å $c = 16.5151(8)$ Å $V = 707.16(5)$ Å^3 $Z = 3$
Space group	$R\bar{3}m$ (No. 166)
Data collection	
Temperature (K)	293(2)
λ (Mo$K\alpha$)	0.71073Å
Crystal shape, size	Distorted rhombohedron, $135 \times 95 \times 75$ μm
$2\theta_{max}$ (°)	61.02
Reflection range	$-9 \leq h \leq 9$; $-10 \leq k \leq 7$; $-15 \leq l \leq 23$
Total no. reflections	1716
No. unique reflections	293
No. refls. $F_o > 4\sigma F$	287
Absorption correction	$\mu = 11.92$ mm^{-1}
R_{merg} on F^2	0.0160
Refinement	
No. parameters refined	32
R_1, $F_o > 4\sigma F$	0.0112
R_1, all data	0.0116
wR_2 F^2*, all data	0.0263
GOF	1.106
$\Delta\sigma_{min}$, $\Delta\sigma_{max}$ (e/Å^3)	−0.48, 0.43

*$w = 1/\sigma^2\left[\left(F_0^2\right) + (0.0129P^2 + 1.68P)\right]$,
$P = \left[2F_c^2 + Max\left(F_0^2, 0\right)\right]/3$.

the Natural History Museum of Los Angeles County. Unit-cell parameters refined from the powder data using Chekcell (Laugier & Bochu, 2004) are $a = 7.064(2)$, $c = 16.5986(6)$ Å and $V = 707.16(5)$ Å^3, which are in good agreement with those obtained from the single-crystal study (see below).

6. Crystal structure determination

The single-crystal study was completed using a Bruker X8 Apex II single-crystal diffractometer at the Department of Chemistry, University of British Columbia. A distorted rhombohedral crystal with the dimensions $135 \times 95 \times 75$ μm was used for collection of intensity data at 293 K (Table 3). The intensity data were processed with the Bruker Apex program suite, with data reduction using the SAINT program (Bruker, 2005) and absorption correction by the multi-scan method using SADABS (Bruker, 2005). No twinning was observed.

The crystal structure of arsenoflorencite-(La) was refined in space group $R\bar{3}m$ (No. 166), using SHELXL–97 (Sheldrick, 2008) with the starting coordinates of plumbogummite (Mills *et al.*, 2009b). The La atom was fixed on the origin as indicated for florencite-(Ce) (Kato, 1990). In later stages of the refinement, La was taken off the origin, but this resulted in the refinement becoming unstable. There is no indication that La is located off the origin in an icosahedrally coordinated site as is the case for Pb members of the supergroup, and La does not usually have a stereoactive lone-pair. The final model for the refinement (with H atom determined) converged to $R_1 = 1.12$ % for 287 reflections [$F_o > 4\sigma F$], and 1.16 % for all 293 reflections. The refined atomic coordinates, site occupancies and displacement parameters are given in Table 4; polyhedral bond distances in Table 5, and a bond-valence analysis in Table 6.

6.1. Description of the structure

Arsenoflorencite-(La) has a typical rhombohedral alunite-type structure (*e.g.*, Blount, 1974). The structure consists of layers of corner-sharing AlO_6 octahedra and AsO_4 tetrahedra, stacked along *c* (Fig. 5). The La atoms lie on the origin between the layers. The octahedra share corners via OH anions, O3, to form a planar network of triangular clusters, encompassing hexagonal voids. Such networks are often described as hexagonal tungsten bronze (HTB) layers (*e.g.*, Grey *et al.*, 2006). The apical O anions, O2, of the triangular groupings of octahedra are shared with the AsO_4 tetrahedra.

Table 4. Atomic coordinates and displacement parameters (Å^2) for arsenoflorencite-(La).

Atom	x	y	z	U_{eq}	U_{11}	U_{22}	U_{33}	U_{23}	U_{13}	U_{12}
La	0.0	0.0	0.0	0.00728(11)	0.00815(12)	0.00815(12)	0.00555(15)	0.0	0.0	0.00408(6)
Al	0.5	0.0	0.5	0.0055(3)	0.0057(3)	0.0044(4)	0.0060(4)	0.0001(3)	0.00004(13)	0.0022(2)
As	0.0	0.0	0.31492(2)	0.00478(13)	0.00472(14)	0.00472(14)	0.00488(19)	0.0	0.0	0.00236(7)
O1	0.0	0.0	0.58543(14)	0.0113(5)	0.0117(7)	0.0117(7)	0.0105(11)	0.0	0.0	0.0059(4)
O2	0.20482(11)	−0.20482(11)	−0.05460(8)	0.0100(3)	0.0117(5)	0.0117(5)	0.0090(6)	0.0005(2)	−0.0005(2)	0.0078(5)
O3	0.12273(11)	−0.12273(11)	0.13701(8)	0.0084(3)	0.0071(4)	0.0071(4)	0.0113(6)	−0.0008(2)	0.0008(2)	0.0037(5)
H1	0.194(2)	−0.194(2)	0.122(2)	0.048(10)						

Site population: Al:Fe 0.89(2):0.11(2); As:P 0.87(2):0.13(2).

Table 5. Polyhedral bond distances (Å) in arsenoflorencite-(La).

La	O2	2.6526(13)	×6
La	O3	2.7118(13)	×6
Al	O3	1.8869(5)	×4
Al	O2	1.9082(13)	×2
As	O1	1.646(2)	
As	O2	1.6753(13)	×3
O3	H1	0.90(3)	

Table 6. Bond-valence analysis for arsenoflorencite-(La).

	La	Al/Fe	As/P	H	$\Sigma_a v$
O1			1.33	0.21	1.54
O2	0.27(↓×6)	0.48(↓×2) (→×2)	1.23(↓×3)		1.98
O3	0.23(↓×6)	0.51(↓×4)		0.79	2.04
$\Sigma_c v$	3.03	3.01	5.00	1.00	

Using the parameters of Brese & O'Keeffe (1991) and Ferraris & Ivaldi (1988).

The XO_4 tetrahedron in the alunite structure-type has one short apical *X*–O1 distance and three longer *X*–O2 distances. In arsenoflorencite-(La), these distances are 1.646(2) and 1.6753(13) Å, respectively, giving a mean <*X*–O> of 1.668 Å. The average bond length is slightly shorter than expected for fully occupied As, consistent with that site being partially occupied by P, in the ratio 0.87:0.13, as indicated by the chemical analyses.

The BO_6 octahedron in the alunite structure-type has two long *B*–O2 distances and four short *B*–O3 distances. In arsenoflorencite-(La), these distances are 1.8869(5) and 1.9082(13) Å, respectively, giving a mean <*B*–O> of 1.894 Å. The refined site occupancy of $Al_{0.89}Fe_{0.11}$ matches the empirical formula well.

The La site lies on the origin and has six equivalent bonds to O2 and six equivalent bonds to O3. In arsenoflorencite-(La), these distances are 2.6526(13) and 2.7118(13) Å, respectively, giving a mean <La–O> of 2.682 Å. The site occupancy refines to 0.98, indicating that the average weight of the site approximates La. There was no change in *R*-value when site occupancy factor values were fixed to the average microprobe data; however, since the microprobe data show a wide range of concentrations of the minor elements substituting for La, the actual occupancies of the minor elements cannot be calculated.

The H1 atom could be accurately determined, as is the case for the majority of alunite-supergroup members. In arsenoflorencite-(La), it forms a O3–H1 . . . O1 bond with the hydrogen distance 0.90(3) Å and an O–O distance of 2.725 Å, categorised as a weak hydrogen bond (Libowitzky & Beran, 2004). The contribution to the BVS is 0.79 *vu* to O3 and 0.21 *vu* to O1, which leaves O1 undersaturated (Table 6). It has often been speculated that a second hydrogen bond exists within the structure (*e.g.*, Blount, 1974, in crandallite); however, as is the case

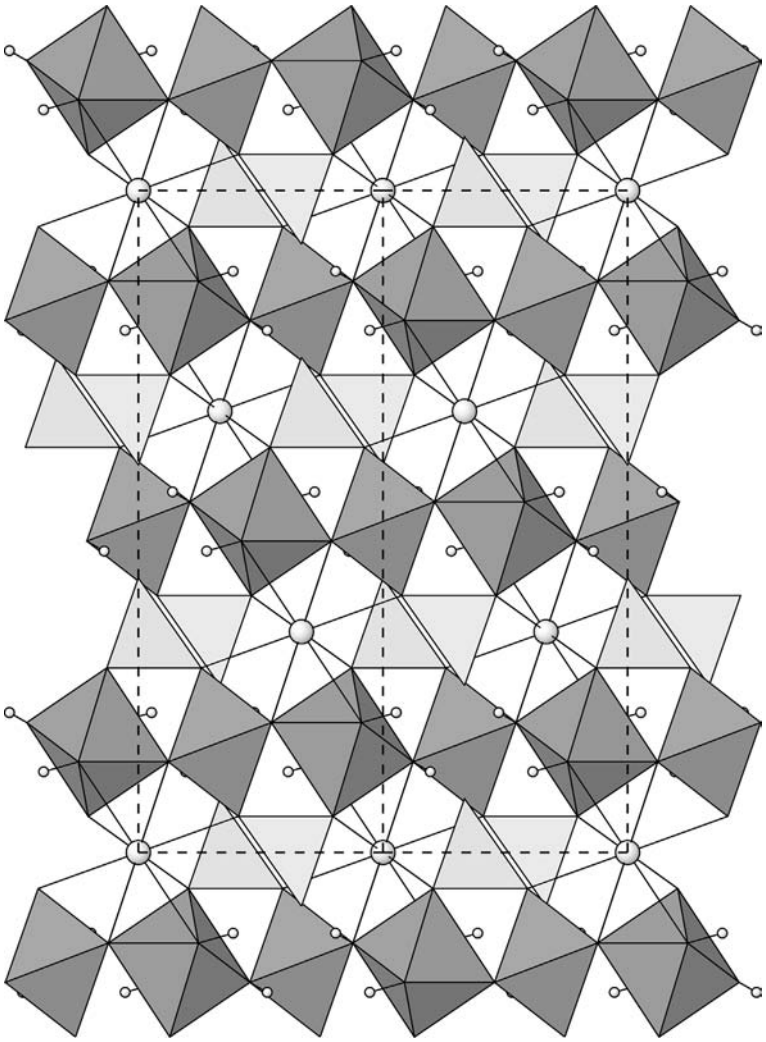

Fig. 5. Crystal structure of arsenoflorencite-(La) viewed down [110] with the *c* axis vertical. La(REE) atoms are large spheres and H atoms are small spheres.

for all alunite-supergroup members, it is uncertain what the hydrogen bonding scheme actually is. The O1 must be partially protonated; however since both O2 and O3 both have formal valences close to 2, clarification of the hydrogen bonding scheme is impossible. Partial occupancy of H1 may be one mechanism to satisfy bond-valence requirements.

7. Discussion

Several geochemical factors present in the Maldynyrd area in the Early Paleozoic contributed to the formation of arsenoflorencite-(La). Initially, strongly oxidising conditions during the formation of the Cambrian crust immobilised Ce. Ce^{3+} was oxidised to Ce^{4+} with the formation of cerianite-(Ce) and/or sorption of oxidised Ce^{4+} onto silicates. As a result of the fractionation of Ce, the REE mineralogy of the region shows La and Nd anomalies, resulting in several new or rare species.

During later events, the conditions changed from oxidising to reducing. Under these later conditions, Ce was further reduced, mobilized and took part in mineral formation together with other REEs. Such reducing environments are characterised by the presence of Fe^{2+} and the dominance of magnetite over hematite. In oxidising environments, primary fractionation was preserved and we observe REE-selective minerals together with hematitisation of the original rocks. Commonly, we observe the results of mixing of these two ''pure'' cases in the co-existence of REE-selective (with La or Nd anomalies) minerals and minerals with smooth, normal REE distribution.

REE mineral microassociations provide important crystallochemical insights. The redistribution of individual REEs is governed by the coordination of the crystallographic sites in the mineral phases and the ionic radii of the individual lanthanoids, such that the most stable (lowest energy) crystalline phases are formed.

An illustration of the last factor is provided by the arsenoflorencite-(La)–chernovite-(Y) pair from different grains of

Table 7. Chemical composition of arsenoflorencite-(La)–chernovite-(Y) pairs.

	1	2	3	4	5	6	7	8
P_2O_5	4.68	2.40	6.66	2.16	4.40	2.03	4.17	7.24
As_2O_5	32.32	34.93	38.24	35.29	40.36	35.41	40.53	37.14
V_2O_5	0.00	0.00	0.00	0.00	0.00	0.00	0.76	0.00
Al_2O_3	25.75	25.57	0.00	25.81	0.00	25.75	0.00	0.00
Fe_2O_3	0.80	0.26	0.00	0.00	0.00	0.00	0.00	0.00
Y_2O_3	0.00	0.00	36.61	0.00	31.73	0.00	35.08	35.53
La_2O_3	15.84	17.61	0.00	17.87	0.00	17.28	0.00	0.00
Ce_2O_3	4.27	5.82	0.00	6.92	0.00	7.46	0.00	0.00
Pr_2O_3	1.43	1.39	0.00	1.11	0.68	1.11	0.00	0.00
Nd_2O_3	3.80	2.84	5.74	1.70	6.95	1.70	4.94	2.15
Sm_2O_3	0.00	0.00	3.72	0.00	3.60	0.00	3.66	2.97
Eu_2O_3	0.00	0.00	0.00	0.00	0.00	0.00	0.00	0.75
Gd_2O_3	0.00	0.00	4.64	0.00	5.99	0.00	5.32	6.94
Tb_2O_3	0.00	0.00	0.00	0.00	1.51	0.00	1.54	0.78
Dy_2O_3	0.00	0.00	3.98	0.00	4.62	0.00	3.92	4.76
Er_2O_3	0.00	0.00	0.00	0.00	0.00	0.00	0.00	1.63
CaO	0.83	0.00	0.00	0.00	0.00	0.00	0.00	0.00
SrO	1.08	0.00	0.0	0.00	0.0	0.0	0.0	0.00
Sum	90.80	90.82	99.59	90.86	99.84	90.74	99.92	99.89
H_2O_{calc}	9.15	9.13	–	9.12	–	9.10	–	–
Total	99.95	99.95	99.59	99.98	99.84	99.84	99.92	99.89
ΣREE	25.34	27.66	54.69	27.60	55.08	27.55	54.46	55.51

Analysis 1: grain of arsenoflorencite-(La) without inclusions of chernovite-(Y) (Fig. 3a); analyses 2–3, 4–5 and 6–7 are of arsenoflorencite-(La) (2, 4, 6) with inclusions of chernovite-(Y) (3, 5, 7) (Fig. 3b–d, respectively); analysis 8 is of later-generation chernovite-(Y) (Fig. 3d).
1 – $[(La_{0.56}Ce_{0.15}Nd_{0.13}Pr_{0.05})_{\Sigma 0.89}Sr_{0.06}Ca_{0.09}]_{\Sigma 1.04}(Al_{2.91}Fe_{0.06})_{\Sigma 2.97}(As_{1.62}P_{0.38})_{\Sigma 2.00}O_{8.00}(OH)_{5.86}$,
2 – $(La_{0.64}Ce_{0.21}Nd_{0.10}Pr_{0.05})_{\Sigma 1.00}(Al_{2.97}Fe_{0.03})_{\Sigma 3.00}(As_{1.80}P_{0.20})_{\Sigma 2.00}O_{8.00}(OH)_{6.00}$,
3 – $(Y_{0.76}Nd_{0.08}Gd_{0.06}Dy_{0.05}Sm_{0.05})_{\Sigma 1.00}(As_{0.78}P_{0.22})_{\Sigma 1.00}O_{4.00}$,
4 – $(La_{0.65}Ce_{0.25}Nd_{0.06}Pr_{0.04})_{\Sigma 1.00}Al_{3.00}(As_{1.82}P_{0.18})_{\Sigma 2.00}O_{8.00}(OH)_{6.00}$,
5 – $(Y_{0.68}Nd_{0.10}Gd_{0.08}Dy_{0.06}Sm_{0.05}Tb_{0.02}Pr_{0.01})_{\Sigma 1.00}(As_{0.85}P_{0.15})_{\Sigma 1.00}O_{4.00}$,
6 – $(La_{0.63}Ce_{0.27}Nd_{0.06}Pr_{0.04})_{\Sigma 1.00}Al_{3.00}(As_{1.83}P_{0.17})_{\Sigma 2.00}O_{8.00}(OH)_{6.00}$,
7 – $(Y_{0.74}Nd_{0.07}Gd_{0.07}Dy_{0.05}Sm_{0.05}Tb_{0.02})_{\Sigma 1.00}(As_{0.84}P_{0.14}V_{0.02})_{\Sigma 1.00}O_{4.00}$,
8 – $(Y_{0.74}Gd_{0.09}Dy_{0.06}Sm_{0.04}Nd_{0.03}Er_{0.02}Eu_{0.01}Tb_{0.01})_{\Sigma 1.00}(As_{0.76}P_{0.24})_{\Sigma 1.00}O_{4.00}$.

our specimen (Table 7 and Fig. 4). The highest concentrations of Nd are observed in arsenoflorencite-(La) grains devoid of chernovite-(Y) inclusions. When Nd increased in chernovite-(Y), the coexisting arsenoflorencite-(La) became depleted in Nd. The incorporation of Nd into the smaller coordination polyhedra of the chernovite structure-type apparently is preferred (of lower energy) over the larger 12-fold coordination observed in the florencite structure-type. The existence of arsenoflorencite-(La) in the specimen reflects the interaction of geochemical and crystallochemical aspects of REE fractionation.

Crystallisation of arsenoflorencite-(La) exhausted the reserve of LREE in solution, resulting in an increase in concentration of HREE. As a result, the REE minerals formed later than arsenoflorencite-(La) within the paragenetic sequence are enriched with intermediate and heavy REE (Table 7, analysis 8).

Acknowledgements: We thank Editor Sandro Conticelli, Associate Editor Luca Bindi and referee Frédéric Hatert for helpful comments on the manuscript. NSERC Canada is thanked for a Discovery Grant to Mati Raudsepp. Part of this study was funded by the John Jago Trelawney Endowment to the Mineral Sciences Department of the Natural History Museum of Los Angeles County. We are also grateful to S.V. Surenkov for providing his field materials for study.

References

Blount, A.M. (1974): The crystal structure of crandallite. *Am. Mineral*., **59**, 41–47.

Brese, N. & O'Keeffe, M. (1991): Bond valence parameters for solids. *Acta Crystallogr*., **B47**, 192–197.

Bruker (2005): *SAINT, SADABS* and *SHELXTL*. Bruker AXS Inc., Madison, WI, USA.

Dutrizac, J.E. & Jambor, J.L. (2000): Jarosites and their applications in hydrometallurgy. *in* ''Sulfate Minerals: Crystallography, Geochemistry, and Environmental Significance'', C.N. Alpers, J.L. Jambor, D.K. Nordstrom, eds. *Rev. Mineral. Geochem*., **40**, 405–452.

Ferraris, G. & Ivaldi, G. (1988): Bond valence vs bond length in O ... O hydrogen bonds. *Acta Crystallogr*., **B44**, 341–344.

Grey, I.E., Birch, W.D., Bougerol, C., Mills, S.J. (2006): Unit-cell intergrowth of pyrochlore and hexagonal tungsten bronze

structures in secondary tungsten minerals. *J. Solid State Chem.*, **179**, 3834–3843.

Grey, I.E., Mumme, W.G., Bordet, P., Mills, S.J. (2008): A new crystal-chemical variation of the alunite-type structure in monoclinic $PbZn_{0.5}Fe_3(AsO_4)_2(OH)_6$. *Can. Mineral.*, **46**, 1355–1364.

Grey, I.E., Mumme, W.G., Mills, S.J., Birch, W.D., Wilson, N.C. (2009): The crystal chemical role of zinc in alunite-type minerals: structure refinements for pure and zincian kintoreite. *Am. Mineral.*, **94**, 676–683.

Jambor, J.L. (1999): Nomenclature of the alunite supergroup. *Can. Mineral.*, **37**, 1323–1341.

Kato, T. (1990): The crystal structure of florencite. *N. Jb. Mineral. Mh.*, **1990**, 227–231.

Klingelhöfer, G., Morris, R.V., Bernhardt, B., Shroder, C., Rodinov, D.S., de Souza, P.A., Yen, A., Gellert, R., Evlanov, E.N., Zubkov, B., Foh, J., Bonnes, U., Kankeleit, E., Gutlich, P., Ming, D.W., Renz, F., Wdowiak, T., Squyres, S.W., Arvidson, R.E. (2004): Jarosite and hematite at Meridiani Planum from Opportunity's Mossbauer spectrometer. *Science*, **306**, 1740–1745.

Kolitsch, U. & Pring, A. (2001): Crystal chemistry of the crandallite, beudantite and alunite groups: a review and evaluation of the suitability as storage materials for toxic metals. *J. Mineral. Petrol. Sci.*, **96**, 67–78.

Kraus, W. & Nolze, G. (1996): *POWDER CELL* – a program for the representation and manipulation of crystal structures and calculation of the resulting X-ray powder patterns. *J. Appl. Crystallogr.*, **29**, 301–303.

Laugier, J. & Bochu, B. (2004): Chekcell: graphical powder indexing cell and space group assignment software, http://www.ccp14.ac.uk/tutorial/lmgp/

Levinson, A.A. (1966): A system of nomenclature for rare-earth minerals. *Am. Mineral.*, **51**, 152–158.

Libowitzky, E. & Beran, A. (2004): IR spectroscopic characterisation of hydrous species in minerals. *in* ''Spectroscopic Methods in Mineralogy'', A. Beran & E. Libowitzky, eds. EMU Notes in Mineralogy, Eötvös University Press, Budapest, **6**, 227–279.

Mills, S.J. & Birch, W.D. (2010): Kolitschit, ein neues Arsenatmineral aus Australien. *Mineralien-Welt*, **21**, 1, 82–85 (In German).

Mills, S.J., Mumme, W.G., Grey, I.E., Bordet, P. (2006): The crystal structure of perhamite. *Mineral. Mag.*, **70**, 201–209.

Mills, S.J., Grey, I.E., Mumme, W.G., Miyawaki, R., Matsubara, S., Bordet, P., Birch, W.D., Raudsepp, M. (2008): Kolitschite, $Pb[Zn_{0.5},\square_{0.5}]Fe_3(AsO_4)_2(OH)_6$, a new mineral from the Kintore opencut, Broken Hill, New South Wales. *Aust. J. Mineral.*, **14**, 63–67.

Mills, S.J., Hatert, F., Nickel, E.H., Ferraris, G. (2009a): The standardisation of mineral group hierarchies: application to recent nomenclature proposals. *Eur. J. Mineral.*, **21**, 1073–1080.

Mills, S.J., Kampf, A.R., Raudsepp, M., Christy, A.G. (2009b): The crystal structure of Ga-rich plumbogummite from Tsumeb, Namibia. *Mineral. Mag.*, **73**, 837–845.

Nordstrom, D.K., Alpers, C.N., Ptacek, C.J., Blowes, D.W. (2000): Negative pH and extremely acidic mine waters from Iron Mountain, California. *Environ. Sci. Technol.*, **34**, 254–258.

Scharm, B., Scharmová, M., Sulovský, P., Kühn, P. (1991): Philipsbornite, arsenoflorencite-(La), and arsenoflorencite-(Nd) from the uranium district in northern Bohemia, Czechoslovakia. *Casopis pro Mineralogii a Geologii*, **36**, 103–113.

Scott, K.M. (1987): Solid solution in, and classification of, gossan-derived members of the alunite-jarosite family, northwest Queensland, Australia. *Am. Mineral.*, **72**, 178–187.

Sheldrick, G.M. (2008): A short history of *SHELX*. *Acta Crystallogr.*, **A64**, 112–122.

Yudovich, Ya.E., Kozyreva, I.V., Shvetsova, I.V., Efanova, L.I., Philippov, V.N. (2000): Manganoan REE-bearing concretions in metamorphic shists at Near-Polar Urals. *Dokl. Akad. Nauk*, **370**, 658–660.

Yudovich, Ya.E., Kozyreva, I.V., Ketris, M.P., Shvetsova, I.V. (2001): Geochemistry of REE in the zone of interformational contact in the Maldynyrd range (Near-Polar Urals). *Geohimiya*, **39**, 3–15.

Received 22 February 2010
Modified version received 24 March 2010
Accepted 6 April 2010